Terr. Atmos. Ocean. Sci., Vol. 23, No. 3, 269-281, June 2012 doi: 10.3319/TAO.2011.12.20.01(T)

The Frequency Distribution of Inter-Event Times of $M \geq 3$ Earthquakes in the Taipei Metropolitan Area: 1973 - 2010

Jeen-Hwa Wang[1,*], Kou-Cheng Chen[1], Shiann-Jong Lee[1], Win-Gee Huang[1], Yi-Hsuan Wu[1], and Pei-Ling Leu[2]

[1] *Institute of Earth Sciences, Academia Sinica, Taipei, Taiwan*
[2] *Seismological Center, Central Weather Bureau, Taipei, Taiwan*

Received 9 September 2011, accepted 20 December 2011

ABSTRACT

$M \geq 3$ earthquakes which occurred in the Taipei Metropolitan Area from 1973 through 2010 are used to study seismicity of the area. First, the epicentral distribution, depth distribution, and temporal sequences of earthquake magnitudes are described. The earthquakes can be divided into two groups: one for shallow events with focal depths ranging 0 - 40 km and the other with focal depths deeper than 60 km. Shallow earthquakes are mainly located in the depth range from 0 - 10 km north of 25.1°N, and down to 35 km for those south of 25.1°N. Deep events are located in the subduction zone, with a dip angle of about 70°. Three statistical models, the gamma, power-law, and exponential functions, are applied to describe the single frequency distribution of inter-occurrence times between two consecutive events for both shallow and deep earthquakes. Numerical tests suggest that the most appropriate time interval for counting the frequency of events for statistical analysis is 10 days. Results show that among the three functions, the power-law function is the most appropriate for describing the data points. While the exponential function is the least appropriate to describe the observations, thus, the time series of earthquakes in consideration are not Poissonian. The gamma function is less and more appropriate to describe the observations than the power-law function and the exponential function, respectively. The scaling exponent of the power-law function decreases linearly with an increasingly lower-bound magnitude. The slope value of the regression equation is smaller for shallow earthquakes than for deep events. Meanwhile, the power-law function cannot work when the lower-bound magnitude is 4.2 for shallow earthquakes and 4.3 for deep events.

Key words: Seismicity, Inter-event time, Single frequency, Gamma function, Power-law function, Exponential function

Citation: Wang, J. H., K. C. Chen, S. J. Lee, W. G. Huang, Y. H. Wu, and P. L. Leu, 2012: The frequency distribution of inter-event times of M ≥ 3 earthquakes in the Taipei metropolitan area: 1973 - 2010. Terr. Atmos. Ocean. Sci., 23, 269-281, doi: 10.3319/TAO.2011.12.20.01(T)

1. INTRODUCTION

Taiwan is situated on the converging boundary between the Philippine Sea plate and the Eurasian plate (Tsai et al. 1977; Wu 1978; Lin 2002). The former moves northwestward with a velocity of about 8 cm yr^{-1} (Yu et al. 1997). The Philippine Sea plate has subducted underneath the Eurasian plate in northern Taiwan, where the Taipei Metropolitan Area (TMA) is located. This converging between the two plates causes high seismicity in the Taiwan region (Wang et al. 1983; Wang 1998; Wang and Shin 1998). The TMA is the political, economic, and cultural center of Taiwan. Hence, it is essential to closely monitor and prepare for regional seismic risk mitigation. For this purpose, the seismicity of the area must be carefully investigated. A description about the geology of the TMA can be found in several articles (e.g., Wang-Lee and Lin 1987; Chang et al. 1998; Teng et al. 2001; Wang et al. 2006) and will not be recapped here.

From 1972 to 1991, the Taiwan Telemetered Seismographic Network (TTSN), which was sponsored by the National Science Council (NSC), was operated by the Institute of Earth Sciences (IES), Academia Sinica to monitor local and regional earthquakes. This network consists of 24 stations, each equipped with a vertical high-gain and analog velocity seismometer. The earthquake magnitude used by

* *Corresponding author*
E-mail: jhwang@earth.sinica.edu.tw

the TTSN was the duration magnitude. Wang (1989a) described this network in detail. Since 1991, old seismic network stations of the Central Weather Bureau (CWB) have been upgraded and many new stations were added to form a new CWB Seismic Network (CWBSN). In 1992 the TTSN was merged into the CWBSN. The earthquake magnitude of the earthquake catalogue has been unified to be the local magnitude. A detailed description about the CWBSN can be found in Shin (1992) and Shin and Chang (2005), only some simple statements are given below. At present, the CWBSN consists of 72 stations, each equipped with three-component velocity seismometers. The seismograms are recorded in both high- and low-gain forms. This network provides high-quality digital earthquake data to the seismological community.

Although seismicity in the TMA is relatively lower than most other seismically active areas in Taiwan, numerous earthquakes still occur in or near the TMA (Hsu 1961, 1971; Wang 1998; Wang et al. 2006). During the Emperor Kanshi period (1661 - 1722) of the Chin Dynasty, an event might have occurred in this area in April or May 1694, resulting in an earthquake-induced lake and destruction of aboriginal houses (Hsu 1983a, b). From historical documents of damages, the magnitude of this event was estimated to be 7 by Hsu (1983b) and Tsai (1985). A detailed description concerning historical earthquakes can be found in Wang et al. (2006). On 15 April 1909, an M 7.3 earthquake took place at 80-km depth beneath the area, causing casualties of 9 death, 51 injuries, 122 houses collapsed, and 1054 houses damaged (Hsu 1961). Lin (2005a) reported that seismicity underneath the Taipei Basin, which was usually low, began to increase slightly during the construction but rose sharply upon the completion of the Taipei 101 building. Astonishingly, two felt earthquakes occurred beneath the completed building leading to debates about building-induced seismicity.

Several researchers (e.g., Tsai et al. 1977; Wu 1978; Wang et al. 1983, 2006; Wang and Shin 1998; Lin 2002) observed that below the TMA there are shallow (0 - 40 km) earthquakes in the crust and deep (> 60 km) events in the Wadati-Benioff subduction zone. Tsai et al. (1973) found that micro-earthquakes occurred mainly in the southern zone of the Tatun Volcano Group (TVG) where larger events showed normal faulting. The epicentral distributions given by Wang et al. (1983) and Kim et al. (2005) both show lower seismicity in the TMA than other areas in northern Taiwan. Wang (1988) evaluated a higher b-value in northern Taiwan than in others. Kim et al. (2005) also obtained a high b-value in the TGV. Wang et al. (1994) observed that except for the earthquakes in the subduction zone, the events occurred in northern Taiwan are usually shallow. Kim et al. (2005) also obtained similar results for $M > 2$ events occurred during 1973 to 2003. They also found three $M \geq 2.8$ normal-faulting events below the TVG. Chen and Yeh (1991) observed that most micro-earthquakes ($0.2 \leq M < 3.0$) in the TVG were located at depths shallower than 10 km and showed normal faulting. Lin et al. (2005) found that the earthquakes occurred underneath the TVG are located mainly at the depth range 2 - 4 km. Konstantinou et al. (2007) observed that all $M < 2.8$ events have a focal depth less than 6 km. Hence, high b-value, shallow focal depth, and normal faulting in the TVG may be due to high geo-temperature from past volcanic activities. Based on the concept proposed by Scholz (1990), these studies imply that the seismogenic zone below the TVG would be thinner than others. Wang et al. (2006) investigated the epicentral distribution, depth distribution, and temporal sequences of $M \geq 4$ earthquakes occurred during 1973 - 2005. Shallow earthquakes are mainly located in depth range from 0 - 10 km north of 25.1°N, and down to 35 km in depth for those south of 25.1°N. After 1988, no $M \geq 4$ shallow event was located within this area. Deep events occurred more or less uniformly during the study time period. The annual number of shallow earthquakes decreased with time from 1973 to 1988, and varies year from year for deep events. They also applied the FR/QP transition model to interpret the depth distribution of shallow earthquakes.

Experience on seismic risk mitigation learned from the TMA can be applied not only to other urban areas in Taiwan, but also in other seismically active regions around the world. However, previous studies of seismicity in the TMA didn't produce sufficient information adequate for the purpose of mitigating seismic risks. Thus, more studies must be doneImportantly, the exploration of the characteristics of inter-event time between two consecutive earthquakes is of considerable interest. The time series of earthquakes occurring in an area is like that shown in Fig. 1. The inter-event time between two consecutive events n and $n + 1$ is denoted by T_n. The frequency distribution of T_n is a significant character of earthquakes (Wang and Kuo 1998). This work will focus on studies of statistical models describing the inter-event time for $M \geq 3$ earthquakes occurring in the area between 1973 - 2010.

2. DATA

From shallow earthquakes occurred in the TMA during 1973 to 1984, Wang (1988) obtained $b = 1.33 \pm 0.13$ in the magnitude range 1.8 - 3.3. For the eastern part of TMA, Wang (1989b) observed $b = 1.21 \pm 0.01$ for the events in the magnitude range of 2.1 - 4.8 occurred between 1973 to 1985. From shallow earthquakes occurred in the TVG during 1973 to 1999, Kim et al. (2005) estimated $b = 1.22 \pm 0.05$ for the magnitude range 2.1 - 3.5. Their results show that the earthquake data should be completed with $M > 2$ in the study area. However, only $M \geq 3$ earthquakes occurred in the area (from 121.3 to 121.9°E and 24.8 to 25.3°N) during 1973 to 2010 are taken into account due to the following

reasons: (1) the ability of detecting earthquakes with $M < 3$ is lower for deep events than shallow ones; and (2) based on seismic risk mitigation, $M \geq 3$ earthquakes are more significant than $M < 3$ events, because damages caused by $M < 3$ events are usually very small. The earthquake data are retrieved directly from the CWB's data base. The quality of location quality is classified into four ranks, i.e., A, B, C, and D, by the CWB. The information can be found in the CWB's Seismological Bulletin (e.g., CWB 2011). In general the maximum location errors for ranks A, B, and C are about 2 km horizontally and 5 km vertically. The location error essentially increases with focal depth.

2.1 Spatial Distributions of Earthquakes

The epicenters of earthquakes in use are plotted in Fig. 2: open circles for shallow (0 - 40 km) earthquakes and solid circles for deep (> 60 km) events as defined below. Since the location error is smaller than 5 km, the separation of the two groups of events is apparent. Figure 2 shows that deep earthquakes are located mainly to the east of 121°30'E as pointed out by Tsai et al. (1977), who suggested that the longitude of 120°30'E marks the west edge of the subduction zone. Shallow earthquakes have focal depths mainly in the range of 0 - 10 km north of 25.1°N and down to 40 km south of 25.1°N. Wang (1989b) and Wang et al. (2006) also found that the earthquakes can be located down to a depth of 40 km in the eastern part of TMA. The shallow events to the north of 25.1°N are located mainly at the TVG. Wang et al. (1994; 2006) observed that except for the earthquakes in the subduction zone, the events occurred in northern Taiwan are usually shallow. Kim et al. (2005) also obtained similar results.

2.2 Depth Frequency of Earthquakes

Figure 3 shows the depth profile of earthquakes along a north-south profile across the TMA. Obviously, the events can be divided into two groups. The first group is in the upper crust and the other is located at deeper depth associated with the Wadati-Benioff subduction zone. Although the error of focal depth is up to 5 km, the separation of the two groups is apparent. The focal depths of deep events increase from south to north that can be associated with 70° northward dipping subduction zone. Wang and Shin (1998) observed that the subduction zone is concaved downward with an average dip angle of 57° above and 72° below 120 km.

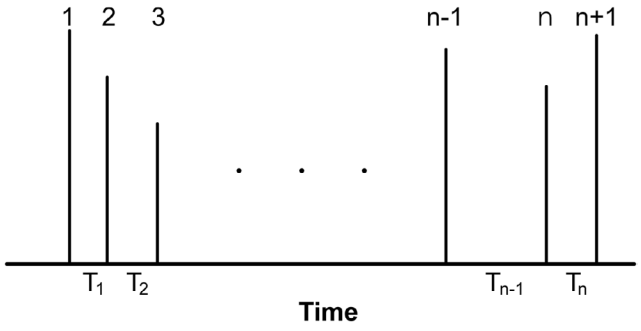

Fig. 1. The occurrence times of earthquakes shown by vertical line segments and the time interval between successive events, T_i (i = 1, ..., n).

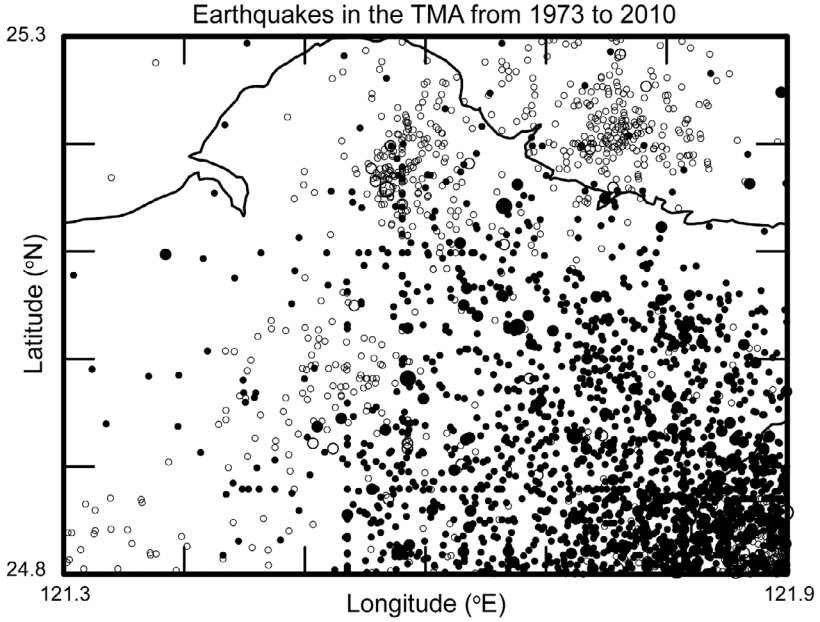

Fig. 2. Epicenters of $M \geq 3$ earthquakes: open and solid circles for shallow (0 - 40 km) and deep (60 - 190 km) events, respectively. Different sized circles show the magnitudes of earthquakes.

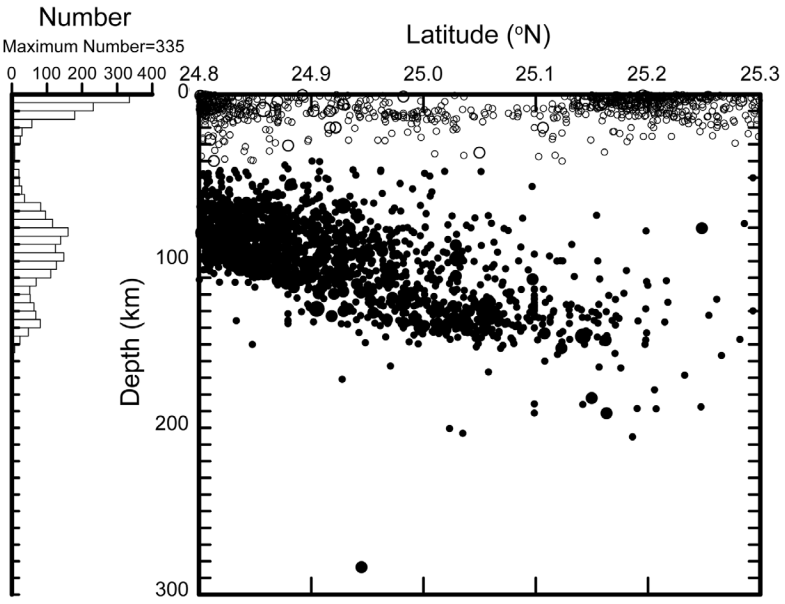

Fig. 3. Right: profile of earthquakes along a specific longitude. Left: depth distribution of numbers of events with a unit of 5 km.

Since the events selected in this study were located only in a section of the subduction zone just underneath the TMA, such a phenomenon cannot be seen here. It is noted that an anomalous earthquake with a focal depth of 283 km beneath the TMA that might be a result of miss-location and thus will not be taken into account in this study.

Included also in Fig. 3 is the depth distribution of numbers of events in a depth interval of 5 km. The shallow and deep earthquakes are defined to be the events located in the depth ranges of 0 - 40 km and 50 - 190 km, respectively. The largest magnitudes are 5.3 and 5.8, respectively, for shallow and deep earthquakes. The largest event occurred on 3 July 1988 is a shallow one with $M = 5.3$. Total numbers of events are 874 and 1697, respectively, for shallow and deep earthquakes. The number of shallow earthquakes has a peak in the depth range from 0 to 5 km and then decreases with depth, while there are several peaks for deep events. It is noted that during the study period, five earthquakes with focal depths deeper than 140 km all took place after 1986.

2.3 Temporal Variation in Earthquake Magnitudes

Figure 4 shows the time series of earthquake magnitudes: (a) for shallow events and (b) for deep events. The shortest inter-occurrence times are less than 1 day for both shallow and deep earthquakes; while the longest inter-event times between two consecutive events are 925.4 and 108.9 days, respectively, for shallow and deep events. Since some events occurred in a short time interval, e.g., a day, the line segments representing them cannot be clearly separated. Hence, those events are plotted by a line segment with the largest earthquake magnitude. It is obvious that after 1988 only an $M > 4$ shallow event was located in the TMA. Deep events occurred more or less uniformly throughout the study time period.

3. STATISTICAL MODELS

The frequency distribution of inter-event time, T_n, between two consecutive events is usually constructed on the basis of either the discrete frequency or the cumulative frequency. For the frequency-magnitude relation, its scaling exponent is generally assumed to be independent on either the selection of single frequency or cumulative frequency. However, the results obtained by Main (1996) from seismic observations and those by Wang (1995) from numerical simulations show a difference in the scaling exponent estimated from the discrete frequency and that from the cumulative frequency. The difference also exists for the inter-occurrence time. Utsu (1984) used the cumulative frequency to evaluate model parameters for the recurrences of earthquakes in several seismic areas in Japan. In this paper, only the discrete frequency distribution of inter-occurrence times is considered, because the probability to have earthquakes occurred in a time span from t to $t + \delta T$ is commonly used for evaluations of seismic hazards. To describe the frequency distribution, the gamma, power-law, and exponential functions are taken into account. These three functions are briefly explained below.

3.1 Gamma Function

The gamma function is a component in various probability-distribution functions characterized by a shape pa-

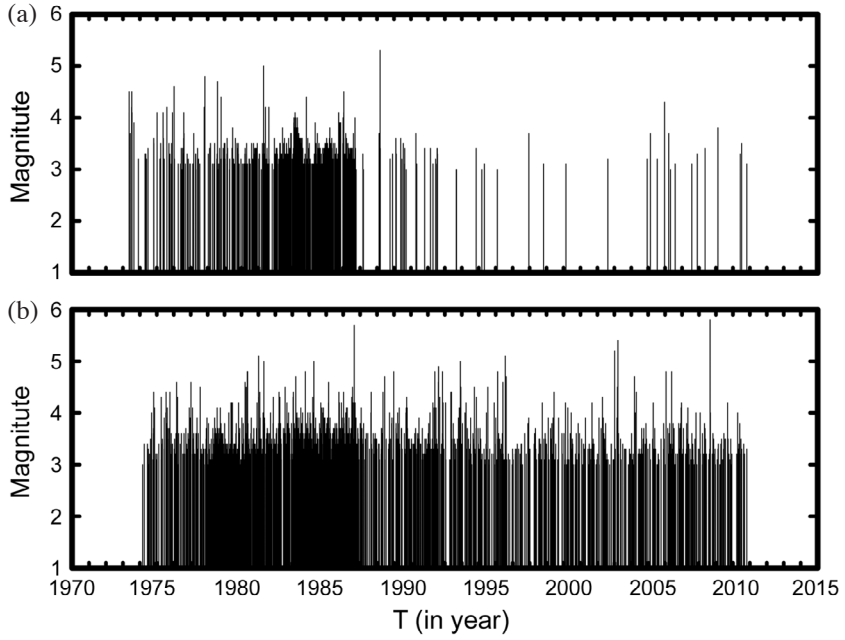

Fig. 4. Time sequences of magnitudes of $M \geq 3$ earthquakes: (a) for shallow events and (b) for deep events.

rameter "A," a scale parameter "a," and a characteristic time "t_0" in the following form:

$$G(t) = A(t/t_0)^{-a+1}\exp(-t/t_0) \quad (1)$$

This function is an extrapolation of the gamma function described in Papoulis (1984). The parameter t_0 merely reflects the units of measurement, while the parameter a controls the shape of the distribution. For $a < 1$, the distribution is a reverse J-shaped curve, for $a = 1$ the distribution is exponential, and for $a > 1$ the distribution has a peak at $t = (a - 1)t_0$. For large t, the term $\exp(-t/t_0)$ dominates, giving the distribution an approximately exponential tail. Equation (1) is a special form of the general gamma function having the following form of $G^*(t) = A(t/t_0)^{-a+1}\exp(-\lambda t/t_0)$ (cf. Main 1996) when $\lambda = 1$. The general gamma function exhibits power law scaling at small time intervals, but with a tail at large time intervals that may either continue this trend right up to the maximum value ($\lambda = 0$), have an exponential tail ($\lambda > 0$), or lead to a 'characteristic' peak near the largest time interval ($\lambda < 0$). This generic behavior is similar to the subcritical ($\lambda > 0$), critical ($\lambda = 0$) and supercritical ($\lambda < 0$). It is obvious that Eq. (1) exhibits subcritical behavior. To simplify the exponent, we let α be $a - 1$. Hence, Eq. (1) becomes $G(t) = A(t/t_0)^{\alpha}\exp(-t/t_0)$. In the following, α rather than $a - 1$ will be estimated.

3.2 Power-Law Function

A power law is a type of mathematical relationship between two quantities. When the frequency of an event varies as a power of some attributes of that event, the frequency is said to follow a power law. For instance, the number of cities having a certain population size is found to vary as a power of the size of the population, and hence follows a power law. The power-law function is characterized by a shape parameter "A," a scale parameter "n," and a characteristic time "t_0" in the following form:

$$P(t) = A(t/t_0)^{-n} \quad (2)$$

3.3 Exponential Function

The property of a Poisson process in time is that inter-event times between consecutive events are exponentially distributed, so that the distribution of inter-event times has the form

$$E(t) = A\exp(-t/t_0) \quad (3)$$

where A and t_0 are the shape parameter and the characteristic time, respectively. It is remarkable that when $t > t_0$, $E(t)$ is approximate to $G(t)$.

Chi-square (χ^2) statistics (cf. Press et al. 1986) will be applied to compare the observed data with the hypothetical curve. Chi-square is defined as $\chi^2 = \sum_i [y_i - y(x_i; a_1, ..., a_m)/\sigma_i]^2$ ($i = 1, ..., N$), where $a_1 ... a_m$ are model parameters and σ_i is the standard deviation of a data point (x_i, y_i). If the measurement errors are normally distributed, with a constant standard deviation (i.e., $\sigma_1 = \sigma_2 = ... = \sigma_N = \sigma$), then the chi-square statistics will give maximum likelihood estimations of the model parameters. On the other hand, if the errors

are not normally distributed, then the estimations are not maximum likelihood. Nevertheless, the statistics may still be useful in the practical application. In this study, we do not know the exact distribution function to interpret the measurement errors. A normal distribution with a standard deviation of $\sigma_i = 1$ for the measurement errors is considered. Hence, we will essentially obtain the maximum likelihood estimations in this study. It is noted that the χ^2 test for goodness of fit is an approximate test and valid only for large samples. The chi-square probability (denoted by p), which gives a quantitative measure for the goodness-of-fit of the model, can be computed by using an incomplete gamma function (cf. Press et al. 1986). If the chi-square probability is large, the goodness-of-fit is reliable. The computing code for chi-square fitting developed by Press et al. (1986) is used in this study.

In order to perform least-square regression for Eqs. (1) - (3) in the following computations, the natural logarithmic values of the two sides of those equations are taken. Hence, Eq. (1) becomes

$$\ln[G(t)] = a_{0g} + a_{1g}t + a_{2g}\ln(t) \tag{4}$$

where $a_{0g} = \ln(At_0^{\alpha})$, $a_{1g} = -1/t_0$, and $a_{2g} = -\alpha$; Eq. (2) becomes

$$\ln[P(t)] = a_{0p} + a_{1p}\ln(t) \tag{5}$$

where $a_{0p} = \ln(A)$ and $a_{1p} = -n$; and Eq. (3) becomes

$$\ln[E(t)] = a_{0e} + a_{1e}t \tag{6}$$

where $a_{0e} = \ln(A)$ and $a_{1e} = -1/t_0$. So, the least-squared fitting and the values of coefficients of equations and chi-square are estimated based on the natural logarithmic forms rather than the original ones.

4. RESULTS

In order to calculate a single frequency, it is necessary to select an appropriate time unit. First, three time units, ΔT, i.e., 1, 10, and 20 days, are tested. Thus, the single frequencies are counted in 1, 2, ..., n days when ΔT = 1 day; in 10, 20, ..., 10n days when ΔT = 10 days; and in 20, 40, ..., 20n days when ΔT = 20 days. The numbers of data points are: 89 and 60, respectively, for shallow and deep events when ΔT = 1 day; 28 and 11, respectively, for shallow and deep events when ΔT = 10 days; and 21 and 6, respectively, for shallow and deep events when ΔT = 20 days. Obviously, the number of data points decreases with increasing ΔT and is larger for shallow events than for deep ones, even though the number of events in use is smaller for shallow earthquakes than for deep ones. This suggests that the χ^2 test would not work well for deep events when ΔT = 20 days. Results are displayed by open circles in Fig. 5 (for ΔT = 1 day), Fig. 6 (for ΔT = 10 days), and Fig. 7 (for ΔT = 20 days): Fig. 7a for shallow earthquakes and Fig. 7b for deep events. The inferred gamma, power-law and exponential functions are shown by the dashed, solid, and dotted lines, respectively. Practical calculations show that for shallow earthquakes,

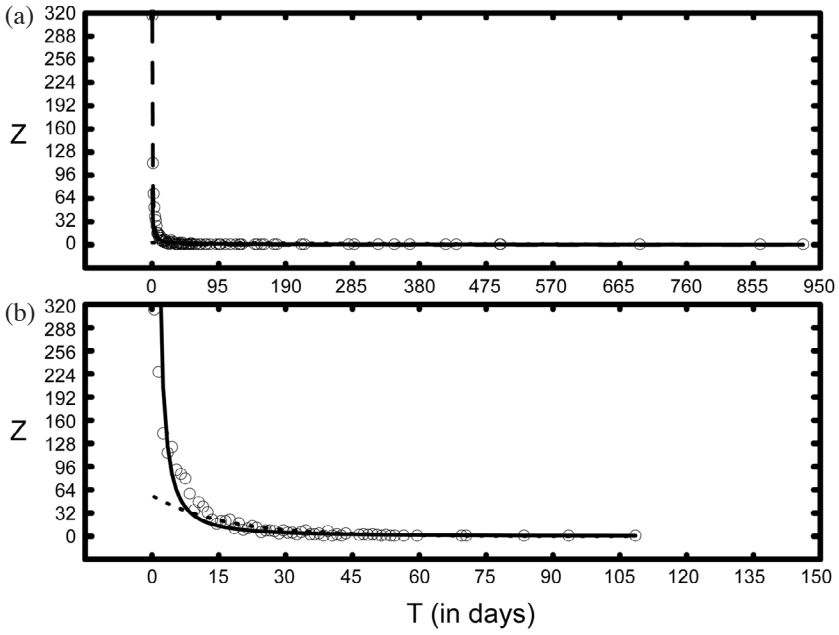

Fig. 5. The plot of frequency (N) versus time (T) for $M \geq 3$ earthquakes with ΔT = 1 day: (a) for shallow events and (b) for deep events and the inferred function: solid line for the power-law function, dashed line for the gamma line, and dotted line for the exponential function.

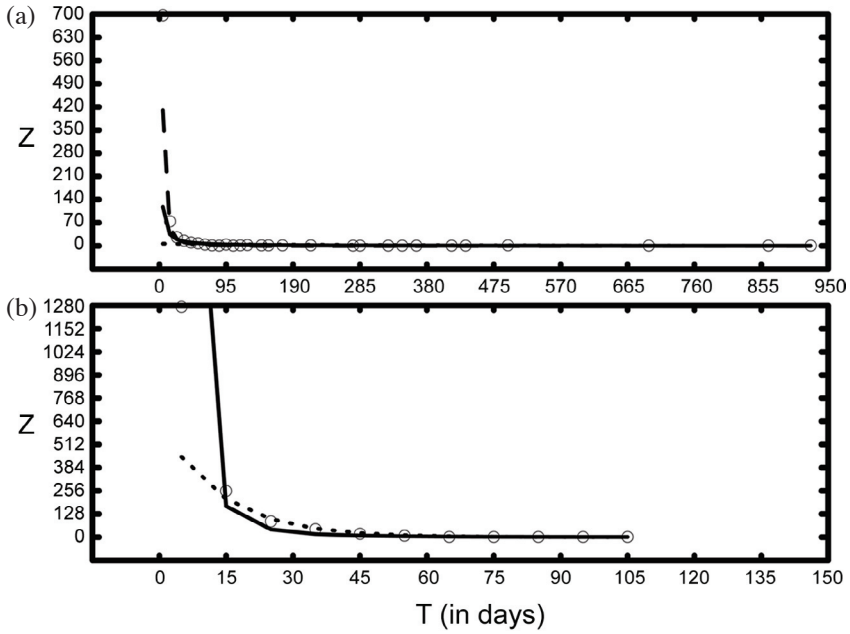

Fig. 6. The plot of frequency (N) versus time (T) for $M \geq 3$ earthquakes with $\Delta T = 10$ days: (a) for shallow events and (b) for deep events and the inferred function: solid line for the power-law function, dashed line for the gamma line, and dotted line for the exponential function.

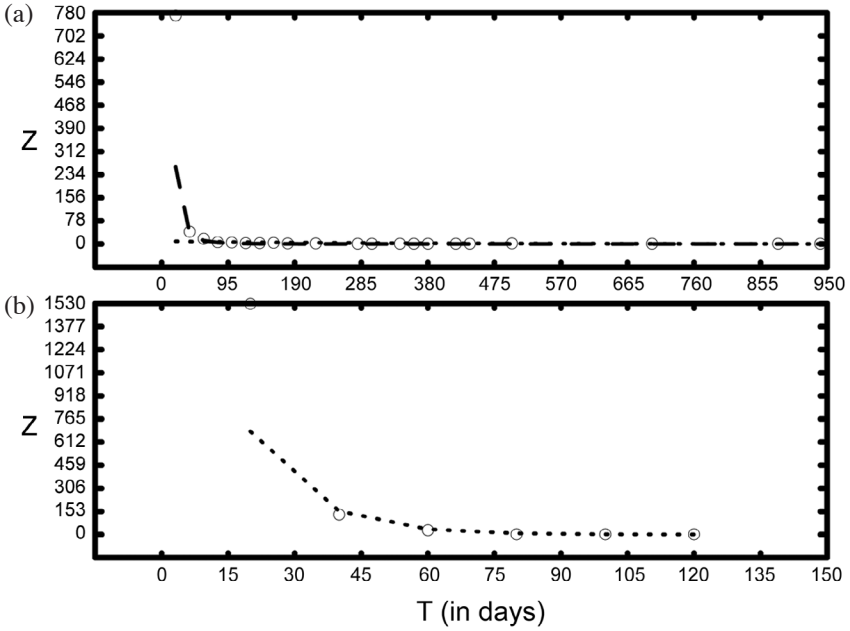

Fig. 7. The plot of frequency (N) versus time (T) for $M \geq 3$ earthquakes with $\Delta T = 20$ days: (a) for shallow events and (b) for deep events and the inferred function: solid line for the power-law function, dashed line for the gamma line, and dotted line for the exponential function.

the patterns of data points for the three values of ΔT are peculiar due to the presence of an abnormally large peak at $T = 1$, 10, and 20 days plus very small frequencies at large T. Nevertheless, the three lines related to the inferred functions are close to one another. For deep earthquakes, the pattern of data points is better. The number of data points is very small when $\Delta T = 20$ days. This phenomenon also exists for $\Delta T > 15$ days. However, the gamma function cannot be inferred for the three cases, because the estimated value of t_0 in Eq. (1) is negative and unreasonable. The numbers of data points, values of model parameters of Eqs. (4) - (6), their standard errors, χ^2, and p are given in Table 1, where the values of model parameters of the gamma function for deep events are absent. The related functions inferred from data are shown in Table 2. For the three time units and two depth ranges, the values of χ^2 and p are, respectively, the

largest and smallest suitable for the exponential function. This means that the exponential function is the least appropriate to describe the statistical property of data points. This situation is more remarkable for shallow earthquakes than for deep events. Since the number of data points when ΔT = 20 days is small, we assume that the appropriate time unit is 10 days for data analysis. In the following studies only ΔT = 10 days is taken into account.

For the purpose of comparison, the three functions are also inferred from $M \geq 4$ earthquakes with ΔT = 10 days. Practical tests suggest that like $M \geq 3$ events, the distributions of data points are quite peculiar, with the presence of an abnormally large peak at the first point plus very small frequencies at others. Unlike the case for $M \geq 3$ with ΔT = 10 days, the lines associated with the respective inferred functions slightly separate and the model parameters of the gamma function for deep events can be evaluated. Meanwhile, it is not appropriate to infer the three functions from the frequency distributions when ΔT = 20 days, because the numbers of data points are too small. For deep earthquakes, the pattern of data points is better than that for $M \geq 3$ and the lines associated with the respective inferred functions are

Table 1. The values of parameters of statistical models, their standard deviations, χ^2, and p for $M \geq 3$ shallow (S) and deep (D) earthquakes when ΔT = 1, 10, and 20 days. The numbers in parenthesis after "S" and "D" are those of data points in use.

	ΔT = 1 day		**ΔT = 10 days**		**ΔT = 20 days**	
	S (89)	**D (60)**	**S (28)**	**D (11)**	**S (21)**	**D (6)**
$\ln[G(t)] = a_{0g} + a_{1g}t + a_{2g}\ln(t)$						
a_{0g}	5.1900 ± 0.4167		10.3336 ± 1.3666		13.5744 ± 2.0400	
a_{1g}	0.0048 ± 0.0010		0.0049 ± 0.0015		0.0052 ± 0.0018	
a_{2g}	-1.2591 ± 0.1229	–	-2.0911 ± 0.3331	–	-2.6404 ± 0.4692	–
χ^2	19.6		7.15		30.5	
p	1.0		1.0		1.0	
$\ln[P(t)] = a_{0p} + a_{1p}\ln(t)$						
a_{0p}	3.8792 ± 0.3251	7.2071 ± 0.4566	6.9687 ± 0.8696	15.5830 ± 1.6798	8.8284 ± 1.2045	20.4291 ± 2.7919
a_{1p}	-0.7828 ± 0.0000	-1.6331 ± 0.0010	-1.1751 ± 0.0000	-3.3926 ± 0.0015	-1.4472 ± 0.0000	-4.3025 ± 0.0018
χ^2	44.9	14.9	17.3	3.9	11.4	1.2
p	1.0	1.0	0.899	0.918	0.911	0.873
$\ln[E(t)] = a_{0e} + a_{1e}t$						
a_{0e}	1.1256 ± 0.1274	4.0560 ± 0.2283	1.9270 ± 0.2723	6.8386 ± 0.6467	2.2606 ± 0.3474	8.0088 ± 0.9309
a_{1e}	-0.0027 ± 0.0001	-0.0616 ± 0.0112	-0.0034 ± 0.0015	-0.0744 ± 0.0302	-0.0038 ± 0.0018	-0.0741 ± 0.0473
χ^2	125.0	33.7	46.5	68.7	34.7	1.2
p	0.005	0.982	0.008	0.651	0.015	0.749

Table 2. The inferred gamma, power-law, and exponential functions for $M \geq 3$ shallow (S) and deep (D) earthquakes when ΔT = 1, 10, and 20 days.

	ΔT = 1 day	**ΔT = 10 days**	**ΔT = 20 days**
$G(t)$			
S	$0.215\ \exp(-t/209)(t/209)^{-1.26}$	$0.447\ \exp(-t/206)(t/206)^{-2.09}$	$0.740\ \exp(-t/129)(t/129)^{-2.64}$
D	Cannot be estimated	Cannot be estimated	Cannot be estimated
$P(t)$			
S	$48.4t^{-0.78}$	$1060.0t^{-1.18}$	$6.83 \times 10^3 t^{-1.45}$
D	$1350.0t^{-1.63}$	$5.9t^{-3.36}$	$7.45 \times 10^8 t^{-4.30}$
$E(t)$			
S	$3.08\ \exp(-t/366.0)$	$6.87\ \exp(-t/269.0)$	$9.59\ \exp(-t/2650.0)$
D	$57.70\ \exp(-t/16.2)$	$9.33 \times 10^2\ \exp(-t/13.4)$	$3.01 \times 10^3\ \exp(-t/13.5)$

close to one another. The numbers of data points, values of model parameters of Eqs. (4) - (6), their standard errors, χ^2, and p from the data sets with $M \geq 3$ and $M \geq 4$ are given in Table 3. The inferred gamma, power-law, and exponential functions are given in Table 4.

5. DISCUSSION

Since the time period of data used in this study is not overly long, the temporal variation in events, especially for those with $M \geq 4$, does not seem to be capable of representing complete seismic behavior of the area. From Fig. 4, neither a positive nor negative correlation can be found between the two time sequences of shallow and deep earthquakes. Earthquakes are expected to form clusters (cf. Kanamori 1977). However, the degree of clustering is lower for shallow earthquakes than for deep events as shown in Fig. 4. After 1988, only a few shallow events happened. Some of them caused remarkable shaking in the TMA (cf. Lin 2005a). For deep earthquakes, the annual number varies from year to year. However, there was an abnormally large number of events in 1986 that may be correlated temporally with the occurrence of an M 7.8 earthquake offshore of the city of Haulien. Such coincidence in time may suggest that a large number of small deep events beneath the TMA may be triggered remotely by a large earthquake in the leading edge of the subduction zone. However, seismicity beneath the TMA was normal after the occurrence of an M 7 earthquake offshore Haulien in 2003. After the 1999 M = 7.6 Chi-Chi earthquake, seismicity was also normal in the TMA, even though the aftershock activity was very high in many areas in Taiwan (cf. Lin 2005b). Therefore, whether the seismicity in the TMA can or cannot be triggered remotely by a large distant earthquake is still in debate.

From Table 1, we can see that the number of data points decreases with increasing ΔT. Small ΔT would be better than large ΔT for producing a large number of data points. As shown earlier in Figs. 5 - 7, the distributions of data points for shallow earthquakes are quite peculiar that abnormally large peaks occurred at T = 1, 10, and 20 days plus very small frequencies for T > 1, 10, and 20 days. These phenomena are not so remarkable in the patterns for deep earthquakes. Hence, it is clear that the pattern of data points for deep earthquakes is better than shallow events. This might be due to a fact that there are significantly more deep earthquakes than shallow events suggesting statistical incompleteness of seismic behavior of shallow earthquakes in the study time period. For almost all model parameters, the standard deviations are small. This means that the estimated values of model parameters are acceptable. The value of χ^2 and p are, respectively, the largest and smallest for the exponential function than for others. The value of χ^2 and p for the gamma function are, respectively, smaller and almost equal to those for the power-law function. Nevertheless, the gamma function cannot be inferred for deep earthquakes. Results suggest that among the three functions, the

Table 3. The values of parameters of statistical models, their standard deviations, χ^2, and p for $M \geq 3$, $M \geq 3.5$, and $M \geq 4$ shallow (S) and deep (D) earthquakes when ΔT = 10 days. The numbers in parenthesis after "S" and "D" are those of data points in use.

	$M \geq 3$		$M \geq 4$	
	S (28)	**D (11)**	**S (18)**	**D (32)**
$\ln[G(t)] = a_{0g} + a_{1g}t + a_{2g}\ln(t)$				
a_{0g}	10.3336 ± 1.3666		1.9569 ± 1.0533	5.6333 ± 1.4160
a_{1g}	0.0049 ± 0.0015		0.0002 ± 0.0002	0.0011 ± 0.0020
a_{2g}	-2.0911 ± 0.3331	–	-0.3286 ± 0.2205	-0.9880 ± 0.3506
χ^2	7.15		4.3	7.0
p	1.0		0.997	1.0
$\ln[P(t)] = a_{0p} + a_{1p}\ln(t)$				
a_{0p}	6.9687 ± 0.8696	15.5830 ± 1.6798	1.5151 ± 0.8270	5.0370 ± 0.9390
a_{1p}	-1.1751 ± 0.0000	-3.3926 ± 0.0015	-0.2232 ± 0.0000	-0.8210 ± 0.0002
χ^2	17.3	3.9	4.7	7.0
p	0.899	0.918	0.997	1.0
$\ln[E(t)] = a_{0e} + a_{1e}t$				
a_{0e}	1.9270 ± 0.2723	6.8386 ± 0.6467	0.4339 ± 0.2552	1.7201 ± 0.2798
a_{1e}	-0.0034 ± 0.0015	-0.0744 ± 0.0302	-0.0001 ± 0.0002	-0.0037 ± 0.0002
χ^2	46.5	68.7	6.5	15.0
p	0.008	0.651	0.982	0.990

Table 4. The inferred gamma, power-law, and exponential functions for $M \geq 3$ shallow (S) and deep (D) earthquakes when $\Delta T = 10$ days.

	$M \geq 3$	$M \geq 4$
$G(t)$		
S	$0.447 \exp(-t/206)(t/206)^{-2.09}$	$0.40 \exp(-t/6230)(t/6230)^{-0.33}$
D	Cannot be estimated	$0.35 \exp(-t/877)(t/877)^{-0.99}$
$P(t)$		
S	$1060.0t^{-1.18}$	$4.6t^{-0.22}$
D	$5.9t^{-3.38}$	$154.0t^{-0.82}$
$E(t)$		
S	Cannot be estimated	$1.54 \exp(-t/11200)$
D	$9.33 \times 10^{8} \exp(-t/13.5)$	$5.60 \times 10^{3} \exp(-t/271)$

power-law function is more appropriate to describe the frequency distribution of earthquakes occurring in the TMA. For gamma and exponential functions, χ^2 varies with ΔT, thus showing that an increase or a decrease in ΔT cannot substantially improve the accuracy of the estimated values of model parameters. For the power-law function, χ^2 decreases with increasing ΔT, thus showing that an increase in ΔT can improve the accuracy of the estimated parameters. Nevertheless, an increase in ΔT results in a decrease of data points, thus leading to a decrease in p. Hence, the time unit of $\Delta T = 10$ days is appropriate for counting frequency of seismicity in the TMA.

From Table 2, we can see that for shallow earthquakes, the values of A of the gamma function in Eq. (1) are less than 1 and slightly increasing with ΔT; while the values of t_0 are slightly decreasing with increasing ΔT. However, the gamma function cannot be inferred for deep earthquakes. For shallow earthquakes, the values of A and n in Eq. (2) for the power-law function both increase with ΔT; while for deep events n follows the increasing trend, but not for A. For both shallow and deep earthquakes, the values of A in Eq. (3) for the exponential function increase with ΔT, while those of t_0 change with ΔT with any definite trend. For deep earthquakes, the values of A for the power-law and the exponential functions are abnormally large. This again suggests that it is not appropriate to use $\Delta T = 20$ days for counting the frequency. Figures 5 - 7 also show that the exponential function cannot describe the data points at small T.

Table 3 shows that for shallow and deep earthquakes with two lower-bound magnitudes, the values of χ^2 are larger for the exponential function than for others. Figures 6 and 8 also show that the exponential function cannot describe the data points at small T for $M \geq 4$ earthquakes. This means that the exponential function is the least useful for describing the frequency distribution. The differences of χ^2 and p between the power-law and gamma functions vary with the lower bound magnitude and are larger when $M \geq 3$ and smaller when $M \geq 4$, thus indicating that the two functions play the same role on the description of frequency distribution.

For the Poissonian time series of earthquakes, the frequency distribution of inter- occurrence time between two consecutive events can be represented mathematically by an exponential function. Wang and Kuo (1998) found that the time series of $M \geq 7$ earthquakes in Taiwan, $M \geq 6$ events in the north-south seismic belt of China, and $M \geq 5.5$ events in Southern California can be represented by the exponential function and thus the occurrence of earthquakes in these regions are Poissonian. Since the previous discussion obviously suggests that the exponential function is less appropriate than the power-law function to describe the present observations, and, thus, the two time series of $M \geq 3$ and $M \geq 4$ earthquakes in the TMA are not or less Poissonian. This means that the occurrence of an earthquake is influenced by previous events. Nevertheless, the exponential function would play a more significant role on the time series of $M \geq 4$ earthquakes than on that of $M \geq 3$ events. Since the gamma function includes both power-law and exponential components, the gamma function is less and more appropriate than, respectively, the power-law function and than the exponential function to describe the observations.

Table 4 shows that the scaling exponent, n, of the power-law function is larger for $M \geq 3$ earthquakes than for $M \geq 4$ events. In order to explore the possible variation in the scaling exponent with the lower-bound magnitude, the values of n are also evaluated for three lower-bound magnitudes, i.e., $M = 3.25$, $M = 3.5$, and $M = 3.75$ events. The estimated values of scaling exponent are: (1) $n = 0.95, 0.73$, and 0.40 for $M = 3.25$, 3.5, and 3.75, respectively, for shallow events; (2) $n = 2.47$, 1.91, and 1.24 for $M = 3.25$, 3.5, and 3.75, respectively, for deep events. The plots of the scaling exponent versus the lower-bound magnitude for both shallow and deep events are displayed in Fig. 9. Obviously, the scaling exponent linearly decreases with increasing lower-bound magnitude. The regression equations are

$$n = (4.15 \pm 2.01) + (-0.99 \pm 0.57)M \quad (7)$$

for shallow events and

$$n = (10.83 \pm 5.12) + (-2.53 \pm 1.47)M \quad (8)$$

for deep events. The slope value is smaller for shallow earthquakes than for deep events. The regression lines will intersect the horizontal axis when $M = 4.2$ and 4.3 for Eqs. (7) and (8), respectively. This means that the power-law function cannot interpret the data points and thus seismic behav-

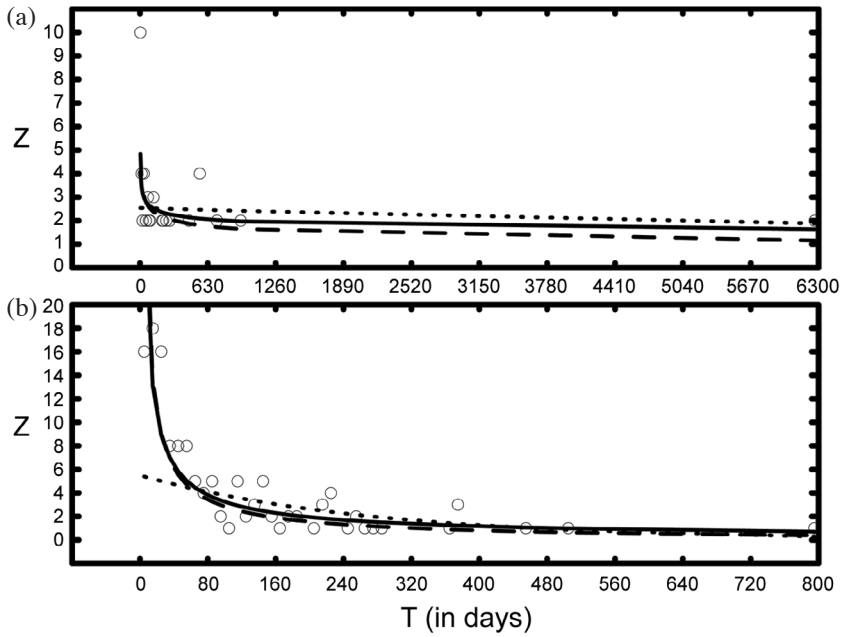

Fig. 8. The plot of frequency (N) versus time (T) for $M \geq 4$ earthquakes with $\Delta T = 10$ days: (a) for shallow events and (b) for deep events and the inferred function: solid line for the power-law function, dashed line for the gamma line, and dotted line for the exponential function.

ior could be Poissonian when the lower-bound magnitude is 4.2 for shallow earthquakes and 4.3 for deep events.

6. CONCLUSIONS

The $M \geq 3$ earthquakes occurred below the Taipei Metropolitan Area between 1973 - 2010 can be divided into shallow (0 - 40 km) and deep (> 60 km) earthquakes, which are located in the crust and subduction zone, respectively. The two groups are separated by an average depth difference of about 20 km. These deep events are associated with the western end of the subducting Philippine plate with a dip angle of about 70°. Shallow earthquakes are located mainly in the depth range 0 - 10 km north of 25.1°N and down to 40 km south of 25.1°N. Three statistical functions, i.e., the gamma, power-law, and exponential functions, are applied to describe the frequency distributions of inter-occurrence times between two consecutive events. Numerical tests suggest that it is most appropriate to use the time unit of $\Delta T = 10$ days for counting the frequency of events for statistical analysis. Results show that among the three functions in use, the power-law function is the most appropriate describing the data points. On the other hand, the exponential function is the least appropriate describing the observations. Thus, the $M \geq 3$ earthquakes are not or less Poissonian. Nevertheless, the exponential function plays a more significant role on $M \geq 4$ earthquakes than on $M < 4$ events. The gamma function cannot interpret deep earthquakes and it is less appropriate and more appropriate respectively, than the power-law function and the exponential function

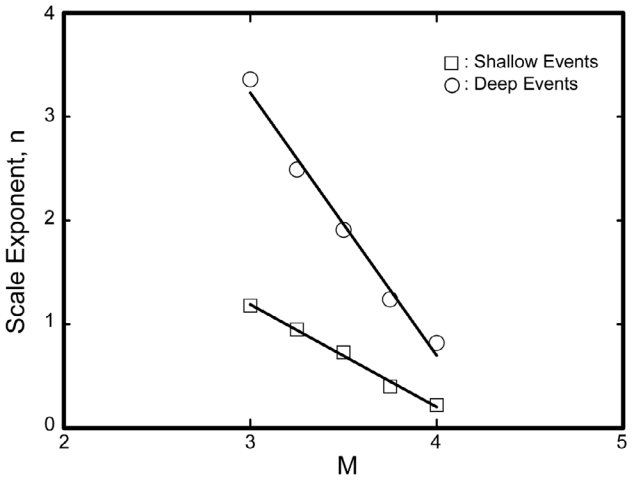

Fig. 9. The plot of scaling exponent, n, of the power-law function versus the lower bound magnitude, M, of earthquakes in use: (a) open squares for shallow events and (b) open circles for deep events. The regression equations are $n = (4.15 \pm 2.01) + (-0.99 \pm 0.57)M$ for shallow events and $n = (10.83 \pm 5.12) + (-2.53 \pm 1.47)M$ for deep events.

to describe the observations for shallow events. The scaling exponent of the power-law function decreases linearly with increasingly lower-bound magnitude. The slope value of the regression equation of the scaling exponent versus lower-bound magnitude is smaller for shallow earthquakes than for deep events. Meanwhile, the power-law function cannot be adopted to interpret the observations when the lower-bound magnitude is 4.2 for shallow earthquakes and 4.3 for deep events.

Acknowledgements The authors would like to thank the Central Weather Bureau for providing earthquake data. They also thank Profs. Y. T. Chen and J. M. Chiu for providing suggestions for improving the article. This work was sponsored by Academia Sinica (Taipei). and the National Science Council under Grant No. NSC100-2119-M-001-015.

REFERENCES

Chang, H. C., C. W. Lin, M. M.Chen, and S. T. Lu, 1998: An Introduction to the Active Faults of Taiwan, Explanatory Text of the Active Fault Map of Taiwan SCALE 1:55000, Central Geological Survey, MOEA, ROC, 103 pp (in Chinese).

Chen, K. J. and Y. H. Yeh, 1991: Gravity and microearthquake studies in the Chinshan-Tanshui area, northern Taiwan. *Terr. Atmos. Ocean. Sci.*, **2**, 35-50.

CWB (Central Weather Bureau), 2011: Seismological Bulletin, January to March, 2010, **57(1)**, p.168, Central Weather Bureau. (in Chinese)

Hsu, H., 1983a: Source materials on the history of natural disasters in Ching Taiwan. Hazards Mitigation S&T Report, 72-01, 5-6 (in Chinese).

Hsu, M. T., 1961: Seismicity of Taiwan (Formosa). *Bull. Earthq. Res. Inst., Tokyo Univ.*, **39**, 831-847.

Hsu, M. T., 1971: Seismicity of Taiwan and some related problem. *Bull. Int. Inst. Seismol. Earthq. Eng., Jpn.*, **8**, 41-160.

Hsu, M. T., 1983b: Estimation of earthquake magnitudes and seismic intensities of destructive earthquakes in the Ming and Ching Eras. *Meteorol. Bull. CWB*, **29**, 1-18 (in Chinese).

Kanamori, H., 1977: The energy release in great earthquakes. *J. Geophys. Res.*, **82**, 2981-2987, doi: 10.1029/JB082i020p02981. [Link]

Kim, K. H., C. H. Chang, K. F. Ma, J. M. Chiu, and K. C. Chen, 2005: Modern seismic observations in the Tatun volcano region of northern Taiwan: Seismic/volcanic hazard adjacent to the Taipei Metropolitan area. *Terr. Atmos. Ocean. Sci.*, **16**, 579-594.

Konstantinou, K. I., C. H. Lin, and W. T. Liang, 2007: Seismicity characteristics of a potentially active Quaternary volcano: The Tatun Volcano Group, northern Taiwan. *J. Volcanol. Geotherm. Res.*, **160**, 300-318, doi: 10.1016/j.jvolgeores.2006.09.009. [Link]

Li, P. H., 1983: The strong earthquake recorders of 1900 to 1972: Re-analysis and occurrence time, spatial distributions study in Taiwan area. Rep. CWB, 49 pp. (in Chinese)

Lin, C. H., 2002: Active continental subduction and crustal exhumation: The Taiwan orogeny. *Terr. Nova*, **14**, 281-287, doi: 10.1046/j.1365-3121.2002.00421.x. [Link]

Lin, C. H., 2005a: Seismicity increase after the construction of the world's tallest building: An active blind fault beneath the Taipei 101. *Geophys. Res. Lett.*, **32**, L22313, doi: 10.1029/2005GL024223. [Link]

Lin, C. H., 2005b: Seismotectonics. In: Wang, J. H., C. Y. Wang, Q. C. Song, T. C. Shin, S. B. Yu, C. F. Shieh, K. L. Wen, S. L. Chung, M. Lee, K. M. Kuo, and K. C. Chang (Eds.), The 921 Chi-Chi Major Earthquake, 249-262, Office of Inter-Ministry S&T Program for Earthquake and Active-fault Research, NSC. (in Chinese)

Lin, C. H., K. I. Konstantinou, W. T. Liang, H. C. Pu, Y. M. Lin, S. H. You. and Y. P. Huang, 2005: Preliminary analysis of volcanoseismic signals recorded at the Tatun Volcano Group, northern Taiwan. *Geophys. Res. Lett.*, **32**, L10313, doi: 10.1029/2005GL022861. [Link]

Main, I., 1996: Statistical physics, seismogenesis, and seismic hazard. *Rev. Geophys.*, **34**, 433-462, doi: 10.1029/96RG02808. [Link]

Press, W. H, B. P. Flannery, S. A. Teukolsky, and W. T. Vetterling, 1986: Numerical Recipes: The Art of Scientific Computing, Cambridge University Press, Cambridge, 818 pp.

Scholz, C. H., 1990: The Mechanics of Earthquakes and Faulting, Cambridge University Press, Cambridge, 439 pp.

Shin, T. C., 1992: Some implications of Taiwan tectonic features from the data collected by the Central Weather Bureau Seismic Network. *Meteorol. Bull. CWB*, **38**, 23-48. (in Chinese)

Shin, T. C. and J. S. Chang, 2005: Earthquake monitoring systems in Taiwan. In: Wang, J. H., C. Y. Wang, Q. C. Song, T. C. Shin, S. B. Yu, C. F. Shieh, K. L. Wen, S. L. Chung, M. Lee, K. M. Kuo, and K. C. Chang (Eds.), The 921 Chi-Chi Major Earthquake, 43-59, Office of Inter-Ministry S&T Program for Earthquake and Active-fault Research, NSC. (in Chinese)

Teng, L. S., C. T. Lee, C. H. Peng, W. F. Chen, and C. J. Chu, 2001: Origin and geological evolution of the Taipei Basin, Northern Taiwan. *West. Pac. Earth Sci.*, **1**, 115-142.

Tsai, Y. B., 1985: A study of disastrous earthquakes in Taiwan, 1683-1895. *Bull. Inst. Earth Sci., Acad. Sin.*, **5**, 1-44.

Tsai, Y. B., H. B. Liaw, and C. C. Feng, 1973: A study of microearthquakes in the Taitun volcanic region in northern Taiwan. Ann. Rept. Inst. Phys., Acad. Sin., 239-250.

Tsai, Y. B., T. L. Teng, J. M. Chiu, and H. L. Liu, 1977: Tectonic implications of the seismicity in the Taiwan region. *Mem. Geol. Soc. China*, **2**, 13-41.

Utsu, T., 1984: Estimation of parameters for recurrence models of earthquakes. *Bull. Earthq. Res. Inst., Univ. Tokyo*, **59**, 53-66.

Wang, C. Y. and T. C. Shin, 1998: Illustrating 100 years of Taiwan seismicity. *Terr. Atmos. Ocean. Sci.*, **9**, 589-

614.

Wang, J. H., 1988: *b* values of shallow earthquakes in Taiwan. *Bull. Seismol. Soc. Am.*, **78**, 1243-1254.

Wang, J. H., 1989a: The Taiwan Telemetered Seismographic Network. *Phys. Earth Planet. Inter.*, **58**, 9-18, doi: 10.1016/0031-9201(89)90090-3. [Link]

Wang, J. H., 1989b: Aspects of seismicity in the southernmost part of the Okinawa trough. *Proc. Geol. Soc. China*, **32**, 79-99.

Wang, J. H., 1995: Effect of seismic coupling on the scaling of seismicity. *Geophys. J. Int.*, **121**, 475-488, doi: 10.1111/j.1365-246X.1995.tb05727.x. [Link]

Wang, J. H., 1998: Studies of earthquake seismology in Taiwan during the 1897-1996 period. *J. Geol. Soc. China*, **41**, 291-336.

Wang, J. H. and C. H. Kuo, 1998: On the frequency distribution of interoccurrence times of earthquakes. *J. Seismol.*, **2**, 351-358, doi: 10.1023/A:1009774819512. [Link]

Wang, J. H., Y. B. Tsai, and K. C. Chen, 1983: Some aspects of seismicity in Taiwan region. *Bull. Inst. Earth Sci., Acad. Sin.*, **3**, 87-104.

Wang, J. H., K. C Chen, and T. Q. Lee, 1994: Depth distribution of shallow earthquakes in Taiwan. *J. Geol. Soc. China*, **37**, 125-142.

Wang, J. H., M. W. Huang, and W. G. Huang, 2006: Aspects of M ≥ 4 earthquakes in the Taipei metropolitan area. *West. Pac. Earth Sci.*, **6**, 169-190.

Wang-Lee, C. M. and T. P. Lin, 1987: The geology and land subsidence of the Taipei Basin. *Mem. Geol. Soc. China*, **9**, 447-464.

Wu, F. T., 1978: Recent tectonics of Taiwan. *J. Phys. Earth*, **2 (Suppl.)**, S265-S299.

Yu, S. B., H. Y. Chen, and L. C. Kuo, 1997: Velocity field of GPS stations in the Taiwan area. *Tectonophyscis*, **274**, 41-59, doi: 10.1016/S0040-1951(96)00297-1. [Link]